Generation of high flux, highly coherent extreme ultraviolet radiation in a gas cell

Lap Van Dao,[a] Sven Teichmann, Jeff Davis, and Peter Hannaford
ARC Centre of Excellence for Coherent X-Ray Science, Centre for Atom Optics and Ultrafast Spectroscopy, Swinburne University of Technology, Melbourne 3122, Australia

(Received 3 December 2007; accepted 15 May 2008; published online 23 July 2008)

We report the generation of extreme ultraviolet radiation with high photon flux (10^{10}–10^{12} photon/cm^2 s), high spatial coherence (up to 0.95), and good spatial beam profile by high-order harmonic generation in various noble gases (argon, neon, and helium) in a gas cell. The photon flux was determined using an extreme ultraviolet spectrometer equipped with a charge-coupled device camera and the spatial coherence was determined from Young double-slit interference fringes. The high-order harmonic emission is confined to just a few orders because of the small phase mismatch in the cut-off region that allows macroscopic phase matching to be satisfied for just a few harmonics in this region. The efficiency and spatial beam profile are studied as a function of gas pressure and geometrical configuration. © *2008 American Institute of Physics*. [DOI: 10.1063/1.2957058]

I. INTRODUCTION

Coherent extreme ultraviolet (XUV) radiation and soft x-ray radiation are currently finding wide application in physics, chemistry, biochemistry, and biology.[1–4] Coherent XUV radiation can now be produced by high-order harmonic generation (HHG) of highly energetic femtosecond laser pulses in noble gases.[5,6] Such a table-top setup can provide a compact source of coherent emission extending down to the water window region,[7] between 2 and 5 nm, a region of great interest for biological applications. High harmonic generation can also provide a source of attosecond pulses for studying ultrafast phenomena.[8,9] Such HHG sources will complement large installations such as x-ray free-electron lasers currently under development. The unique properties of HHG emission present opportunities for new applications in atomic and molecular spectroscopies, condensed matter physics, imaging on the nano-and subnanoscale, and plasma physics. The brightness (which is related to the conversion efficiency from the near-infrared laser light to XUV light), the spatial and temporal coherence properties, the photon energy, and the pulse repetition rate are important properties of the source from the point of view of potential applications. The main challenge for the field at this time is to improve and control the properties of the source.

Significant enhancement in the efficiency of HHG has been achieved by several groups through quasi-phase-matching,[10–15] and the "absorption limit" for which reabsorption limits the effective length of the medium[11] has now been reached. However, the conversion efficiencies depend on the HHG configuration even within the absorption limit, and the ultimate optimization conditions are still far from being fully characterized. It has been shown that the efficiency of the high-order harmonics near the cut-off region can be enhanced, while that of the harmonics in the plateau region is reduced by using self-guided laser beams,[16] hollow waveguides,[13] or gas cells.[17] The conversion efficiency with phase matching was 4×10^{-5} using Xe gas[13] where the phase matching was performed by balancing the dispersions due to neutral atoms, free electrons, and focusing geometry.

Not only the enhancement in the HHG efficiency but also the beam profile and the spatial and temporal coherence are important factors for investigating the generation process and for its applications to, for example, coherent diffraction imaging.[18,19] In principle the spatial and temporal coherence properties of the incident laser are transferred to the generated HHG field. However, the nonlinear polarization induced in the medium is a complex function of space and time, and this can change the coherence of the harmonic beam generated by the high-order nonlinear processes. For many applications, such as coherent diffractive imaging,[19] a monochromatic beam or a beam with a narrow and well-characterized bandwidth is another important requirement of the XUV source. A spectrometer is typically used to select the bandwidth of the radiation; however, the transmission of spectrometers in the XUV region is very low. The generation of just a few harmonics, especially a single harmonic, that can be used directly without a spectrometer would be advantageous for such applications.

In this paper we report high harmonic generation by a freely propagating fundamental beam in a gas cell to obtain the same benefits of homogeneous phase matching as in hollow-core fibers.[14] We also show that a high efficiency, high coherence, and good spatial beam profile can be achieved for a small number of harmonics, e.g., from the 27th to the 33rd harmonic in argon, from the 51st to the 63rd harmonic in neon, and from the 59th to the 81st harmonic in helium.

II. EXPERIMENT

The laser pulses required for HHG are generated by a 1 kHz multistage multipass chirped-pulse amplifier system,

[a]Author to whom correspondence should be addressed. Electronic mail: dvlap@swin.edu.au.

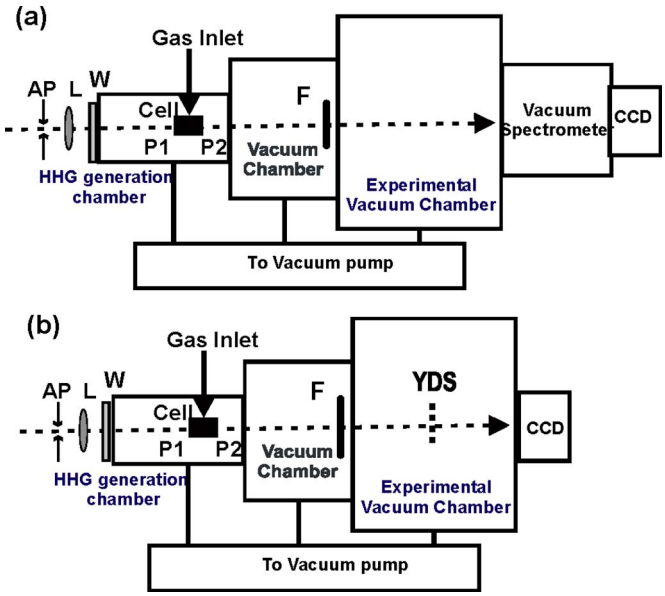

FIG. 1. (Color online) Schematic diagram of the experiment setup for generation and detection of XUV beam (a) for recording the spectrum and (b) for recording the Young double-slit interference fringes [AP: variable aperture; L: focusing lens; W: glass window; P1: entrance pinhole; P2: exit pinhole; F: metal filter (200 μm Al or Zr foil); and YDS: Young double slits].

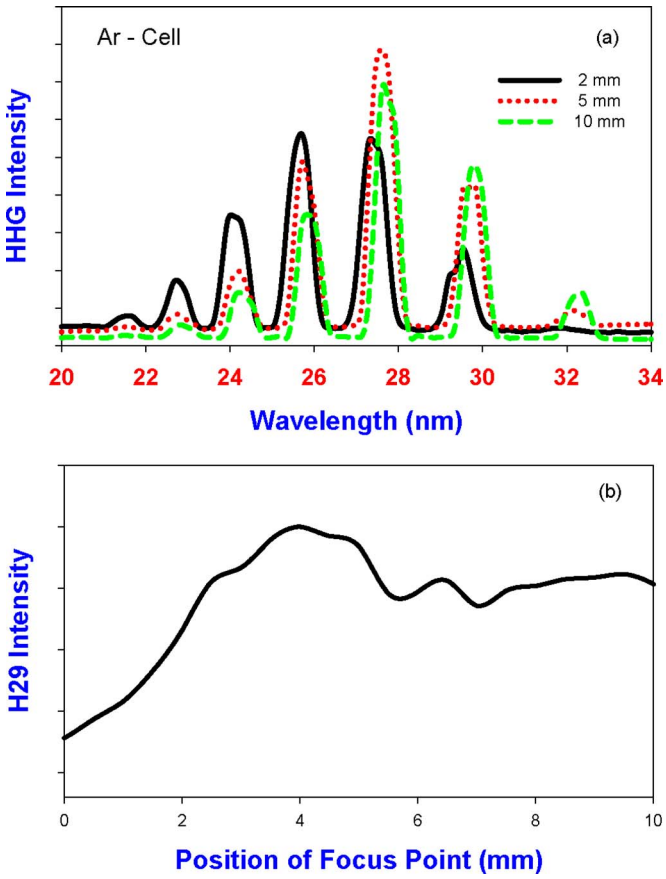

FIG. 2. (Color online) (a) Spectra emitted from an argon gas cell at 25 Torr for different distances between the focus point of the laser beam and the entrance pinhole. (b) Intensity of the 29th harmonic plots vs distance between the focus point of the laser beam and the entrance pinhole of the gas cell. Positive distance indicates that the focus position is in the gas cell.

which produces 5 mJ pulses with a duration of 30 fs centered at 805 nm, beam diameter of 15 mm, and beam quality of $M^2 \sim 1.6$. The experimental arrangement for generation and detection of the XUV radiation is shown in Fig. 1. The laser pulses are focused by a 500 mm focal length lens into a 10 mm long gas cell with 150 μm pinholes at the entrance and exit, which are also used to isolate the vacuum chamber from the gas-filled cell. The beam radius at the focus is about 50 μm and the Rayleigh length is 10 mm. The effective peak intensity at the focus is approximately 5×10^{14}–10^{15} W/cm^2. The experiments show that the diameter of an aperture, which is placed in the path of the laser beam before the focusing lens, has a remarkable influence on the intensity and beam profile of the HHG signal.[20] The influence of the size of the aperture is attributed to the effective f-number, the spatial quality of the laser beam, and the peak intensity in the focus area (truncation). The variation of the aperture introduces phase variations in the laser wavefront that can be used to minimize the mismatch between the laser phase and the intrinsic phase of the harmonics.

We use different gases for this experiment because of their different cut-off regions, and therefore different spectrum ranges can be generated. In the pressure range 10–50 Torr, the spatial profile of the transmitted fundamental beam in the gas cell does not change significantly. Harmonics are not generated when the gas cell is evacuated below 10^{-2} Torr. The pressure in the vacuum chamber outside the 10 mm long gas cell is kept at $<1 \times 10^{-3}$ Torr. The position of the focus point relative to the entrance pinhole can be varied. The high harmonics created on axis or close to the optical axis pass through a 200 nm thick aluminum (Al) or zirconium (Zr) filter, which removes the fundamental beam, and then through a 0.2 mm wide, 20 mm high entrance slit of the XUV spectrometer before being dispersed by a diffraction grating at grazing incidence and detected by a back-illuminated XUV charge-coupled device (CCD). To determine the range of HHG orders, a slit is placed at the exit focal plane of the grating and the angle of the grating is scanned. The spectrally resolved far-field profile of the harmonics is detected along the height of the exit slit. A very broad range of XUV wavelengths (2–80 nm) with high spectral resolution can be detected with a set of four different gratings (150, 300, 600, and 1200 grooves/mm).

III. RESULTS AND DISCUSSION

Typical XUV spectra emitted from an argon gas cell at 25 Torr for three different distances (2, 5, and 10 mm) between the focus point of the laser and the entrance pinhole of the cell are shown in Fig. 2(a), where positive distance indicates that the focus position is in the gas cell. Only a few harmonic orders are detected, and no harmonics are observed in the plateau region despite the intensity of the fundamental laser beam being sufficiently high (5×10^{14}–10^{15} W/cm^2) to produce harmonics in the plateau region.[10,17] It has been shown that for harmonic generation in different length gas cells, the conversion efficiency decreases rapidly with decreasing wavelength because of the phase-velocity mismatch.[17,21] The extent of the phase matching is sensitive to the Gouy phase shift, the density of the gas medium, and

the intensity of the laser pulses, and thus the intensities of the harmonics depend on the focus position, the gas pressure, and the intensity of the laser. Each harmonic is broadened due to propagation effects.[22] The blueshift of the harmonic peaks, which increases slightly with increasing interaction length, is caused by self-phase modulation in the leading edge of the driving pulse and is also observed when a hollow fiber is used.[23,5] The radial variation of the phase for different quantum pathways[17,24] leads to an effective selection of trajectories where the path with the slowly varying phase survives longest during the propagation and provides a clearly resolved spectrum of harmonics.

The difference of absorption coefficients for two harmonics, the 27th (H27) (at ~29.5 nm) and the 31st (H31) (at ~25.8 nm), is large,[17] but we still observe an enhancement for both of these harmonics, which is dependent on the size of the input beam and the position of the focus. In the pressure range 25–50 Torr we do not observe a strong pressure dependence in the intensity of H27 and H31 provided the diameter of the fundamental beam is adjusted for maximum intensity. This indicates that the absorption behaves quite differently in the strong field regime and that it does not influence the phase-matching process. For a long propagation length of HHG in the gas cell (at a distance 2 mm), the influence of the absorption is reflected in the shift in the total spectrum of high harmonic orders.

Figure 2(b) shows the intensity of H29 versus the position of the focus. The size of the aperture is chosen for maximum intensity and good spatial beam profile of the HHG radiation when the focus of the laser beam is positioned at the center of the cell (5 mm). The wave vector k for a light wave propagating in a gas medium can be written as[10]

$$k = 2\pi/\lambda + 2\pi N_{\mathrm{at}} n(\lambda)/\lambda - N_e r_e \lambda,$$

where N_{at} is the density of neutral atoms, $n(\lambda)$ is the linear refractive index per unit neutral atom density, N_e is the density of free electrons, and r_e is the classical electron radius. We note that the contribution from free electrons in the plasma is negative, which allows the opportunity to reduce the phase mismatch when the ratio of N_{at}/N_e is suitably chosen by variation of the laser intensity. The harmonic generation is optimal and enhanced when the difference between the phase velocities of the fundamental and harmonic beams is minimized over the length of the medium. In general, the phase mismatch is also dependent on the wavelengths of the harmonics because the electron density that contributes to the generation of certain harmonics is different.

In the case of propagation in a gas-filled cell, the Gouy phase shift in the fundamental beam over the confocal length can lead to destructive interference between the harmonics created before and after the focus.[25] The propagation term induced by the phase shift of the Gaussian fundamental field is proportional to $-q \arctan(2z/b)$, where z is the propagation distance ($z=0$ at the focus position), b is the Rayleigh length, and q is the harmonic number. The positive dispersion due to the plasma and the negative dispersion due to the neutral argon indicate that the strong enhancement can be attributed to a macroscopic phase matching similar to that produced in a hollow fiber.[17] Self-guiding of the femtosecond pulses occurs as a result of beam convergence due to self-focusing and beam divergence due to multiple photoionization. Variation of the diameter of the input beam can be used to choose an optimal intensity, which fixes the ionization level and the Rayleigh length; thus, the quasi-plane-wave can be guided over long distances.

The intensity dependence of the phase of the dipole moment has a strong influence on the propagation and can lead to strong spatial distortion.[12] The atomic dipole phase depends on the intensity, which varies with propagation distance as $I(z)=I_0/(1+4z^2/b^2)$, where I_0 is the peak intensity. The total phase mismatch of the qth harmonic is $\Delta k_q = (2\pi\omega/c)\, N_{\mathrm{at}}(q n_{q\omega} - n_\omega)$, where $n_{q\omega}$ and n_ω are the refractive indices of the harmonic wave and the fundamental wave, respectively. The refractive indices ($n_{q\omega}$ and n_ω) consist of a linear part and a nonlinear part, which is also a function of the peak laser intensity. The refractive index of neutral argon is strongly intensity dependent because of the high nonlinear refractive index n_2. The extent of the phase matching depends strongly on the position relative to the laser focus because of the contribution of the intensity. The periodic oscillation of the harmonic intensity with gas pressure and interaction length is given by $I_q(z) \sim N_{\mathrm{at}}^2 \sin^2(\Delta k\ z/2)/\Delta k^2$. This provides positive and negative energy transfer between the fundamental wave and the harmonic wave[25] that depends on the phase mismatch Δk. If the two wavelengths are phase matched ($\Delta k \sim 0$), the HHG intensity increases with the length of the interaction medium. For a gas pressure of 25 Torr [Fig. 2(b)], the intensity of H29 first increases quadratically with the length, which is consistent with phase matching, and then there is only a small variation. In the cut-off region (harmonics H21–H31) the complex refractive index (refraction and absorption) is large and strongly dependent on wavelength, and the maximum intensity of H25 and H29 can be obtained at different positions of the focus as shown in Fig. 2(a). The dependence of the linear and nonlinear refractive indices and the absorption on wavelength lead to the generation of only a few harmonics for certain conditions of geometry and laser intensity. The number of harmonics is low, but the conversion efficiency for each harmonic is much higher than when using the gas jet configuration.

The coupling between the laser and HHG fields is limited to the axial direction, and the phase variation along the optical axis can be small in the cut-off region when the variation of phase with laser intensity is small. The intrinsic phase is much more stable for harmonics in the cut-off region than for those in the plateau region, and phase matching can be realized for harmonics near the cutoff.[17] The harmonic spectral distribution, especially the total band width, shows a weak dependence on the interaction length and focus position. The optimal gas pressure is 25–35 Torr in order to compensate for the two significant phase shift mechanisms of these harmonics.

In contrast to argon gas for which the variation of absorption in the wavelength range 25–30 nm is large, the variation of absorption for helium gas in the wavelength range 10–20 nm is relatively small. The number of generated harmonics in the helium gas cell is larger (59th–81st) and the spectrum varies with the focus position [Fig. 3(a)]. The HHG

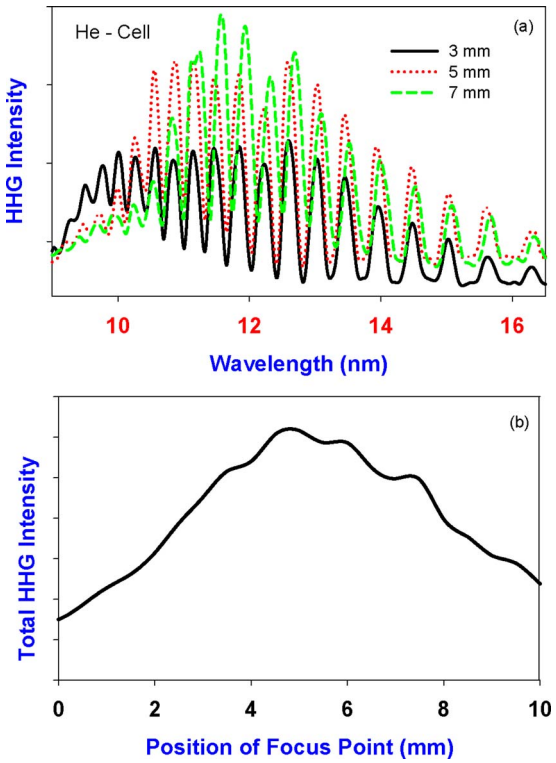

FIG. 3. (Color online) (a) Spectra emitted from a helium gas cell at 20 Torr for different distances between the focus point of the laser beam and the entrance pinhole of the cell. (b) Intensity of all harmonic plots vs distance between the focus point of the laser beam and the entrance pinhole of the gas cell. Positive distance indicates that the focus position is in the gas cell.

intensity decreases on both sides of the optimal position more rapidly, as shown in Fig. 2(b), because the phase mismatch is larger in helium.

The HHG photon number N_{ph} is calculated from the CCD detector signal (PIXIS-XO-1024B, Roper Scientific) directly and after dispersion by the spectrometer using the expression $N_{\mathrm{ph}}=(N_c\eta/QE)(3.65/E_{\mathrm{ph}})$, where N_c is the number of counts per CCD pixel, η depends on the setting of the hardware gain given by the factory, QE is the quantum efficiency of the detector which is nearly constant over the range of photon energies 20–200 eV, and E_{ph} is the photon energy. For argon gas the photon flux is $>2\times10^{12}$ photons/harmonic cm^2 s or $\sim5\times10^{10}$ photons per shot, which is higher than when a capillary is used.[13] For He gas the photon flux is $\sim10^{10}$ photons/harmonic cm^2 s, which is much higher than in a previous study[26] where a photon flux of 5×10^8 photons/s at 12.4 nm in a 5% spectral band was reported.

We have measured the spatial profile of the harmonic beam generated in an Ar gas cell for different focus positions. In this experiment, at a gas pressure of 25 Torr, the optimal spatial profile is smooth and nearly Gaussian with a divergence of about 1 or 2 mrad (for different harmonic orders) when the focus position is about 9 mm from the entrance pinhole [Fig. 4(b)]. A significant change is observed in the case of a short distance between the focus and the entrance pinhole (5 mm) where the beam becomes broad and expands over 2 mrad [Fig. 4(a)]. We could obtain a very good beam quality with narrow divergence by properly controlling the focus position and the gas density.

To study the spatial coherence properties of the HHG radiation, interference fringes from a Young double-slit were measured. The Young double slit consists of two parallel slits with 5 μm width and 100 μm height separated by a distance of 20 μm. The HHG radiation with all harmonics is used to illuminate the double slits, and high contrast interference fringes are obtained as shown in Fig. 5. These interference fringes confirm that only a few harmonics are generated. From the contrast of the interference fringes, the degree of spatial coherence for HHG radiation in an argon gas cell is determined to be about 0.95.

IV. CONCLUSIONS

We have observed enhancement in the photon flux, high spatial coherence, and good beam profile for high-order har-

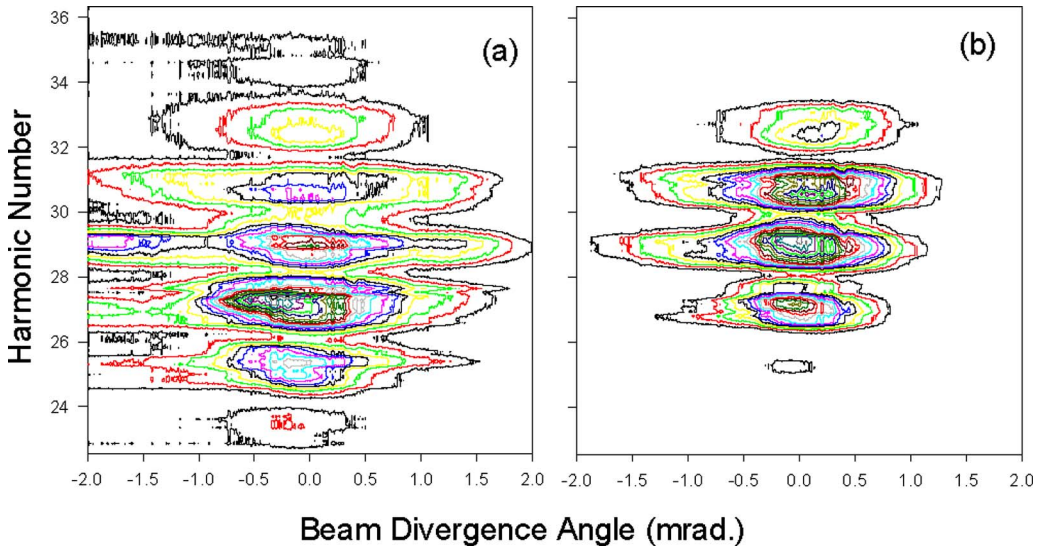

FIG. 4. (Color online) Harmonic far-field spatial profile of HHG radiation from an argon gas cell at 25 Torr for different distances between the focus point of the laser beam and the entrance pinhole of the cell: (a) 5 mm and (b) 9 mm.

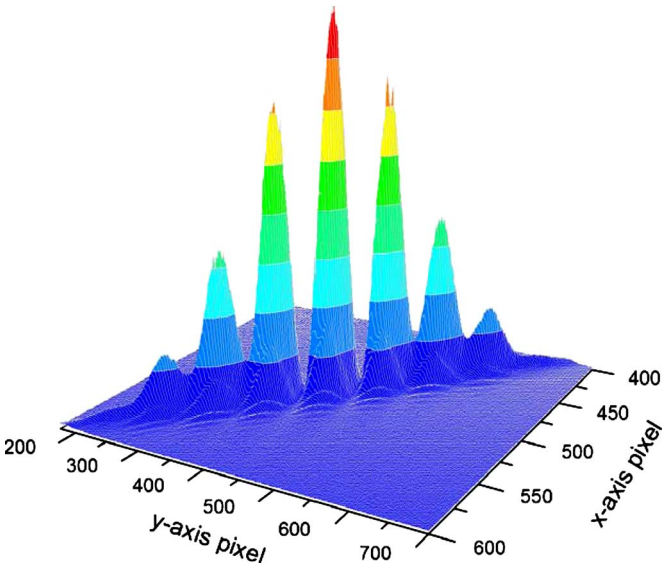

FIG. 5. (Color online) High contrast interference fringes from the Young double slits illuminated with HHG radiation from an argon gas cell.

monic radiation near the cut-off region in a gas cell. This behavior is caused by the small phase mismatch in the cut-off region, allowing macroscopic phase matching to be satisfied for harmonics in this region. The harmonic order yielding the highest intensity is unchanged with gas pressure when a suitable aperture size is chosen. With further increase in the available interaction length, the harmonic signal is reduced because of the strong inhomogeneity of the ionization distribution. The generation of few high-order harmonics in a gas cell can be used as a coherent source of XUV radiation for coherent diffraction imaging.

ACKNOWLEDGMENTS

We thank B. Chen from the University of Melbourne and C. Tran and A. Peele from La Trobe University for providing the Young double slits.

[1]G. Mourou, Z. Chang, A. Maksimchuk, J. Nees, S. V. Bulanov, V. Yu. Bychenkov, T. Zh. Esirkepov, and H. Ruhl, Plasma Phys. Rep. **28**, 12 (2002).
[2]P. Villoresi, P. Ceccherini, L. Poletto, G. Tondello, C. Altucci, R. Bruzzese, C. de Lisio, M. Nisoli, S. Stagira, G. Cerullo, S. De Silvestri, and O. Svelto, Phys. Rev. Lett. **85**, 2494 (2000).
[3]R. A. Bartels, A. Paul, H. Green, H. C. Kapteyn, M. M. Murnane, S. Backus, I. P. Christov, Y. Liu, D. Attwood, and C. Jacobsen, Science **297**, 376 (2002).
[4]M. Hentschel, R. Kienberger, Ch. Spielmann, G. A. Reider, N. Milosevic, T. Brabec, P. Corkum, U. Heinzmann, M. Drescher, and F. Krausz, Nature (London) **414**, 509 (2001).
[5]J. Zhou, J. Peatross, M. M. Murnane, H. C. Kapteyn, and I. P. Christov, Phys. Rev. Lett. **76**, 752 (1996).
[6]J. J. Macklin, J. D. Kmetec, and C. L. Gordon, Phys. Rev. Lett. **70**, 766 (1993).
[7]Z. Chang, A. Rundquist, H. Wang, M. M. Murnane, and H. C. Kapteyn, Phys. Rev. Lett. **79**, 2967 (1997).
[8]P. B. Corkum, N. H. Burnett, and M. Y. Ivanov, Opt. Lett. **19**, 870 (1994).
[9]I. P. Christov, M. M. Murnane, and H. C. Kapteyn, Phys. Rev. Lett. **78**, 1251 (1997).
[10]A. Rundquist, C. G. Durfee, Z. Chang, C. Herne, S. Backus, M. M. Murnane, and H. C. Kapteyn, Science **280**, 1412 (1998).
[11]M. Schnürer, Z. Cheng, M. Hentschel, G. Tempea, P. Kálmán, T. Brabec, and F. Krausz, Phys. Rev. Lett. **83**, 722 (1999).
[12]P. Salières, A. L'Huillier, and M. Lewenstein, Phys. Rev. Lett. **74**, 3776 (1995).
[13]E. Constant, D. Garzella, P. Breger, E. Mével, Ch. Dorrer, C. Le Blanc, F. Salin, and P. Agostini, Phys. Rev. Lett. **82**, 1668 (1999).
[14]C. G. Durfee, A. R. Rundquist, S. Backus, C. Herne, M. M. Murnane, and H. C. Kapteyn, Phys. Rev. Lett. **83**, 2187 (1999).
[15]S. Kazamias, D. Douillet, F. Weihe, C. Valentin, A. Rousse, S. Sebban, G. Grillon, F. Augé, D. Hulin, and Ph. Balcou, Phys. Rev. Lett. **90**, 193901 (2003).
[16]Y. Tamaki, J. Itatani, Y. Nagata, M. Obara, and K. Midorikawa, Phys. Rev. Lett. **82**, 1422 (1999).
[17]K. Midorikawa, Y. Tamaka, J. Itatani, Y. Nagata, and M. Obara IEEE J. Sel. Top. Quantum Electron. **5**, 1475 (1999).
[18]R. L. Sandberg, A. Paul, D. A. Raymondson, S. Hädrich, D. M. Gaudiosi, J. Holtsnider, R. I. Tobey, O. Cohen, M. M. Murnane, H. C. Kapteyn, C. Song, J. Miao, Y. Liu, and F. Salmassi, Phys. Rev. Lett. **99**, 098103 (2007).
[19]B. E. Allman, P. J. McMahon, J. B. Tiller, K. A. Nugent, D. Paganin, A. Barty, I. McNulty, S. P. Frigo, Y. Wang, and C. C. Retsch, J. Opt. Soc. Am. A **17**, 1732 (2000).
[20]S. Kazamias, F. Weihe, D. Douillet, C. Valentin, T. Planchon, S. Sebban, G. Grillon, F. Augé, D. Hulin, and Ph. Balcou, Eur. Phys. J. D **21**, 353 (2002).
[21]E. Takahashi, Y. Nabekawa, T. Otsuka, M. Obara, and K. Midorikawa, Phys. Rev. A **66**, 021802 (2002).
[22]N. H. Shon, A. Suda, Y. Tamaki, and K. Midorikawa, Phys. Rev. A **63**, 063806 (2001).
[23]Y. Tamaki, Y. Nagata, M. Obara, and K. Midorikawa, Phys. Rev. A **59**, 4041 (1999).
[24]M. B. Gaarde, F. Salin, E. Constant, Ph. Balcou, K. J. Schafer, K. C. Kulander, and A. L'Huillier, Phys. Rev. A **59**, 1367 (1999).
[25]P. Balcou, P. Salières, A. L'Huillier, and M. Lewenstein, Phys. Rev. A **55**, 3204 (1997).
[26]E. Seres, J. Seres, F. Krausz, and C. Spielmann, Phys. Rev. Lett. **92**, 163002 (2004).